Photon-Induced Oxidation of Graphene/Ir(111) by SO_2 Adsorption

Stefan Böttcher*, Hendrik Vita, Karsten Horn

Fritz-Haber Institute of the Max-Planck Society, Faradayweg 4-6, 14195 Berlin, Germany

Abstract

We prepare a single layer of graphene oxide by adsorption and subsequent photo-dissociation of SO_2 on graphene/Ir(111). Epoxidic oxygen is formed as the main result of this process on graphene, as judged from the appearance of characteristic spectroscopic features in the C 1*s* and O 1*s* core level lines. The different stages of decomposition of SO_2 into its photo-fragments are examined during the oxidation process. NEXAFS at the carbon K edge reveals a strong disturbance of the graphene backbone after oxidation and upon SO adsorption. The oxide phase is stable up to room temperature, and is fully reversible upon annealing at elevated temperatures. A band gap opening of 330 ± 60 meV between the valence and conduction bands is observed in the graphene oxide phase.

Keywords: Graphene, Graphene Oxide, Functionalization, NEXAFS, XPS, ARPES, Adsorbates, Fragmentation

1. Introduction

Covalent functionalization of graphene, the two-dimensional lattice of hexagonally arranged carbon atoms, has attracted much attention in the past years. For a variety of applications, the introduction of foreign atoms into the graphene lattice [1] or the breaking of the sp^2 configuration of graphene by attaching new atomic species is of interest. Such processes may induce a gap between the valence and conduction bands at the so-called Dirac point in graphene. Possible ways to achieve this are hydrogenation [2, 3] or fluorination [4, 5], yielding band gaps on the order of 3 eV [2, 4, 6]. However, hydrogenated graphene ("graphane") appears to be unstable, while fluorographene requires complex chemical processes. Another element which has been used for covalent functionalization of graphene is oxygen, leading to different modifications of graphene oxide (GrO), a widely discussed precursor for the industrial production of graphene sheets [7]. GrO is commonly referred to as a compound of oxidized graphite sheets, containing a variety of functional groups, e.g. ketones, esters, ethers or hydroxyl groups [7]. Graphene itself can be oxidized in several ways, as for example in wet solutions [8] or by aggressive physical treatments such as hot oxygen atom bombardment[9, 10]. The methods used have a strong influence on the chemical composition, i.e. of the functional groups found in graphene oxide. Oxygen atom bombardment leads almost exclusively to the production of epoxidic oxygen atoms[9, 10]. Epoxides are oxygen atoms bridging two carbon atoms that are linked via a single bond and are likely to be formed on the double bond of graphene, breaking the sp^2 symmetry towards an sp^3 hybridization. The present study aims to provide an alternative, chemical pathway to obtain high quality and selectively oxidized graphene layers; the quality of graphene oxide has turned out to be crucial for the successful preparation of high-quality graphene from graphene oxide. For example, Larcipete *et al.* [11] report that only epoxidic oxygen groups in graphene oxide result in graphene sheets of high quality upon thermal recovery of graphene from GrO.

The preparation of oxidized graphene layers, consisting of mainly epoxidic oxygen has been studied by several groups [9–11]. However, while the preparation method in these publications (oxygen atom bombardment) is a viable pathway, it is also reported to induce defects into the graphene lattice. We have recently presented a method to selectively obtain epoxidic oxygen in graphene through low temperature adsorption and photon-induced decomposition of nitrogen dioxide, NO_2 [12]. This method is less intrusive and thus probably less destructive to the graphene layer, because the reactive oxygen species is prepared not from a hot oxygen source but from adsorbed oxygen containing molecules on the surface at low temperatures. Here we report on the use of a different adsorbate, sulfur dioxide (SO_2), to oxidize a monolayer graphene on Ir(111), yielding a single layer of graphene oxide on Ir(111). We show that this pathway towards oxidation, similar to NO_2, selectively leads to epoxidic oxygen. Adsorption and decomposition of precursors under irradiation may therefore be a general approach towards chemical functionalization of graphene. Graphene oxide thus formed is stable up to room temperature and the oxidation process induces a band gap between the valence and conduction bands. Besides the oxidation and its characteristic spectral features, we observe a strong influence of the decomposition products of SO_2 on graphene, showing that they can interact relatively strongly with graphene and block adsorption sites for oxidation. First we identify the graphene oxide spectral features in the substrate (carbon 1*s*) and adsorbate (oxygen 1*s*) core level photoemission lines. We then discuss the appearance of remaining SO fragments on the surface and their effect on

*Corresponding Author Tel.: +49 30 8413 5620
Email address: boettcher@fhi-berlin.mpg.de (Stefan Böttcher)

graphene. Using NEXAFS, we study the influence of oxidation and the SO fragments on the carbon hybridization state. Finally, the effect of oxidation on the valence and conduction level states of graphene, and the opening of a band gap between these is investigated using angle resolved photoelectron spectroscopy (ARPES).

2. Experimental

The experiments were performed at the UE56/2-PGM-2 beamline of BESSY II, Berlin (Germany). Graphene/Ir(111) was prepared on a clean Ir(111) single crystal surface as described in [12]. The quality of the graphene/Ir(111) sample was verified by means of low energy electron diffraction (LEED), NEXAFS, x-ray photoelectron spectroscopy (XPS), and ARPES. The deposition of SO_2 was performed using a high purity gas source at a partial pressure of $p = 5 \cdot 10^{-8}$ mbar and at a sample temperature of 100 K. This temperature was kept for all measurements unless specified otherwise. NEXAFS spectra were collected at the carbon K absorption edge in the surface sensitive partial electron yield mode (PEY) using a hemispherical detector and Auger electron yield. ARPES measurements contain a 3D data set of photoemission intensity $I(E_{kin}, k_x, k_y)$, where E_{kin} is the kinetic energy of the emitted electrons and k_x and k_y are the two orthogonal components of the in-plane electron wave-vector. The base pressure during measurements was better than $2 \cdot 10^{-10}$ mbar. The average photon flux density of the beamline was around 10^{18} photons/cm^2·s [13]. The photon induced decomposition of SO_2 and the oxidation of graphene/Ir(111) using synchrotron radiation was in general obtained prior to the measurements presented below unless specified otherwise.

3. Results and Discussion

The adsorption of SO_2 and its photodissociation on graphene/Ir(111) is reflected in the carbon 1s photoemission (PE) line as shown in the spectrum in Figure 1, acquired at an excitation energy of 450 eV. The C 1s PE line shows new spectral lines when compared to clean graphene/Ir(111). Apart from the well known [9, 12] graphene (sp^2) component, located at 284.1 eV binding energy (line A) and with a full width at half maximum (FWHM) of 390 meV (pristine graphene/Ir(111) has a FWHM of 350 meV), two new features appear. Line C in Figure 1 is located at 286.2 eV binding energy, and we assign this to the epoxidic component of the graphene oxide formed. The term epoxide refers to an oxygen atom that bridges two carbon atoms, leaving the C-C σ-bond intact; the carbon atoms involved into this chemical group change their electron configuration from sp^2 to sp^3. This distortion of the two-dimensional graphene lattice is carried on further into the graphene lattice: the carbon atoms adjacent to the epoxidic groups also experience an (albeit much smaller) distortion, which leads to a spectral line appearing as a shoulder next to the pristine graphene signal at 284.6 eV binding energy (line B in Figure 1). Both features are in good agreement with literature data on the oxidation

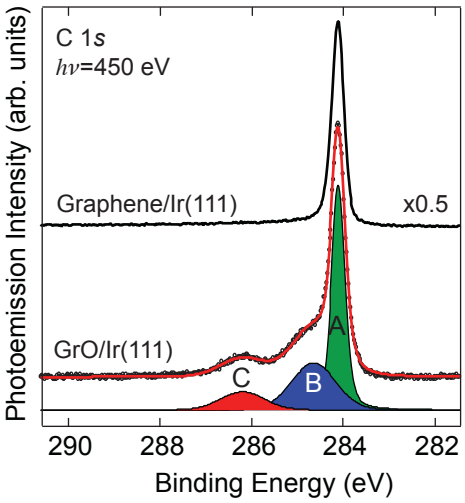

Figure 1: Carbon 1s core level line for graphene/Ir(111), as well as for GrO/Ir(111), obtained from adsorption and photolysis of SO_2 on graphene/Ir(111), acquired at an excitation energy of $h\nu$ = 450 eV. The individual spectral components belong to pristine graphene (A), sp^3 hybridized carbon (B) and epoxidic carbon (C).

of graphene [9, 10, 12]. The single sharp C 1s core level line of pristine graphene on Ir(111) is thus split into three components observed as sp^2-bonded carbon atoms in pristine graphene (A), those carbon atoms driven into an sp^3 configuration by adjacent epoxidic groups (B), and the epoxidic carbon atoms themselves (C). The relative intensities of these peaks are 54:33:13 for A:B:C, the ratio between B and C is 2.5:1. This is relatively large, and we consider that every epoxy group contains two carbon atoms and is surrounded by four carbon atoms which are distorted due to the presence of the epoxidic group (this model assumes that the epoxide group is isolated on the surface). This purely geometrical assumption would lead to an upper limit for the ratio of 2:1 for peak B and C. The observed ratio is thus 25% larger than expected; it is also larger than found in our recent study of NO_2 decomposition, which also results in graphene oxide [12], where we observed an sp^3:epoxide ratio of 1.7:1.

We interpret this observation as a sign that, in graphene oxide preparation by SO_2 adsorption and decomposition, a lower coverage with epoxidic oxygen species is reached than for GrO prepared by NO_2 decomposition [12] or oxygen atom bombardment [9, 10]. The epoxidic component represents only 13% of the integrated C 1s peak intensity, while for NO_2 we observed 23% under similar conditions [12]. Beside the lower concentration of epoxidic oxygen, another possible influence yielding the pronounced rehybridization shoulder B could be that the graphene lattice is much more distorted than the oxidation state suggests, and involves the assumption that the remaining decomposition products may have a strong influence on the graphene backbone as well, leading to a stronger rehybridization of the carbon atoms in graphene.

Figure 2 shows the oxygen 1s (a) and the sulfur 2p (b) core level line spectra for different photon dosages and stages of the experiment. All spectra are fitted by Voigt profiles, using restricted Lorentzian weights to incorporate structural uncertain-

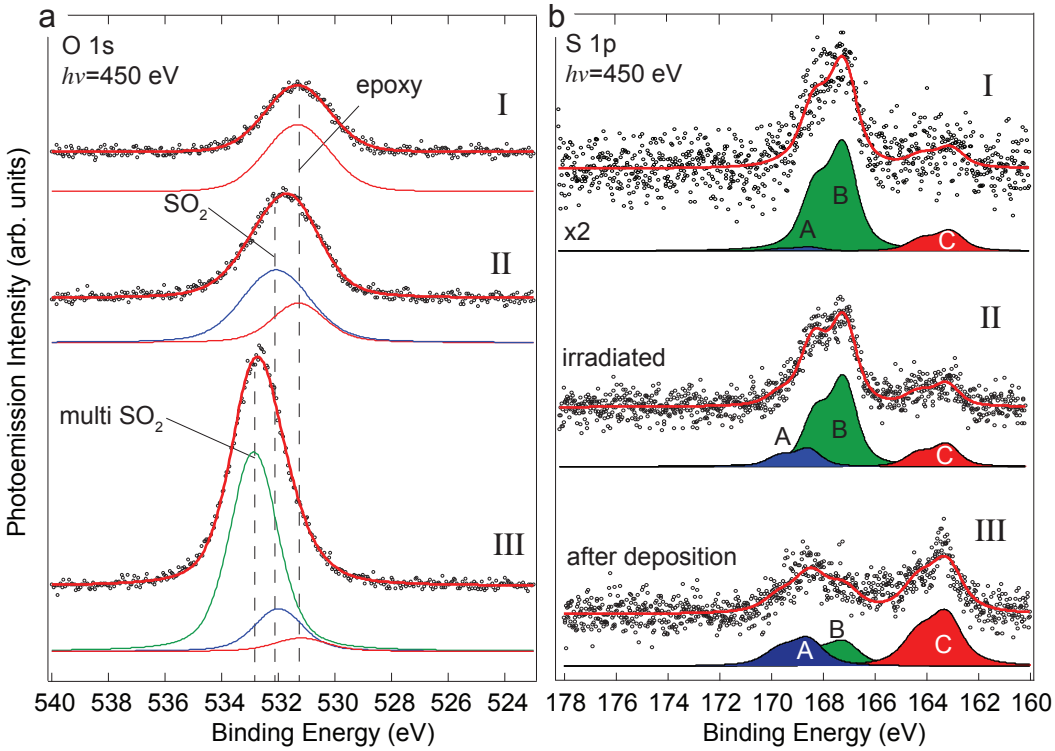

Figure 2: **a:** Oxygen 1*s* core level spectra for graphene/Ir(111) after SO_2 adsorption and irradiation. Spectrum I shows the O 1*s* core level of GrO, while spectra II and III belong to a larger coverage of SO_2 on the surface. Spectrum III is acquired during the irradiation and oxidation process, and spectrum II is obtained after a similar photon dose as spectrum I. **b:** Sulfur 2*p* core level line for the experimental stages described for the O 1*s* core level line. The individual spectral lines correspond to SO_2 (A), SO (B) and elemental sulfur (C).

ties within the Gaussian weight; the background was included in the fits and is removed in the figures for clarity. The sulfur 2*p* core level lines were fitted using a spin-orbit splitting. The individual spectral components (A to C) of the core level lines were used for all fits of the corresponding energy regimes in order to reduce the number of free parameters in the fitting procedure. The left panel of Figure 2 shows the oxygen 1*s* core level line spectra for graphene/Ir(111) after SO_2 adsorption and irradiation. We interpret spectrum I as due to graphene oxide, corresponding to the carbon 1*s* core level shown in Figure 1, obtained by photon irradiation under a photon flux density of approx. $6 \cdot 10^{21}$ photons/cm^2 under an equilibrium pressure of $p(SO_2) = 5 \cdot 10^{-8}$ mbar. In this experiment, only one O 1*s* component is found. The large FWHM of 280 meV may suggest that more than one species of oxygen atoms is present, but we cannot resolve these. The amount of oxygen obtained on the basis of the XPS signal intensity ratio is roughly 1:4 (O 1*s*:C 1*s*), showing a slightly larger amount of oxygen (≈25%) than calculated on the basis of the C 1*s* core level spectral components (Fig. 1), from which we infer that only epoxides are present. A possible explanation for the large O 1*s* line width is that epoxides on different adsorption sites, such as the *atop* and *hollow* regions of graphene/Ir(111) supercell are present [9, 14], but fragments of SO_2 are also possible, as there is more oxygen present on the surface as expected from the C 1*s* core level line alone. Spectra II and III represent an experiment with a larger initial coverage of SO_2 (the O 1*s*:C 1*s* intensity ratio is 1.75:1). III shows the O 1*s* spectrum after the initial coverage and II represents the sample after irradiation with a similar photon dose as for I. The epoxidic O 1*s* component (red) is found in both spectra II and III, in agreement with spectrum I, developing in intensity with subsequent photon irradiation. In addition, two increasing lines appear, which we assign to the first adsorbed SO_2 layer (blue) and multilayers layers of SO_2 on graphene (green). After irradiation (spectrum II) only the first layer of SO_2 is left, together with the grown epoxidic line. Note that spectrum III is acquired during the preparation step (the oxidation was processed by the synchrotron radiation) and may incorporate contributions from the ongoing chemical reaction during every acquisition cycle. However, this uncertainty only affects the intensity of the single components but not the energy. This is especially true for the epoxide groups and first layer SO_2 signals, which exhibit a different intensity compared to spectrum I and II. This discrepancy also results from the fact that the multilayer SO_2 further suppresses the photoemission signal, due to the fact that the photoelectrons have to penetrate an additional molecular layer. We would like to note that no evidence of intercalated oxygen has been observed within the experiments presented here. Intercalated oxygen at defects is possible in principle as we have partly observed it in our recent work [12], and as it is reported in the literature [9, 11]. However, the apparently low damage of the graphene layer by the method presented here appears to suppress the intercalation of oxygen atoms.

The right panel of Figure 2 shows the sulfur $2p$ photoemission lines upon adsorption and decomposition of SO_2. The individual components are interpreted as decomposition products of SO_2 caused by the irradiation. Three components are observed: SO_2 (blue), SO (green) and atomic sulfur (red) [15, 16]. All spectra were fitted using the same set of spin-orbit split Voigt profiles and including the background. The spectra are presented with the background subtracted for clarity. We have restricted ourselves to the same FWHM, spin-orbit splitting and positions for each component in all sulfur $2p$ spectra. Spectrum I corresponds to the C $1s$ (Figure 1) and top O $1s$ lines (Figure 2), e.g. the low initial SO_2 coverage. The majority component is SO, in agreement with earlier observed data from decomposed SO_2 on Pt(111) [15, 16]. Its intensity corresponds to an amount of sulfur of about 5% with respect to the C $1s$ intensity. Besides the SO component, also atomic sulfur and SO_2 are observed in the S $2p$ line. The SO_2 component is taken into account in this spectrum because it appears in the other spectra and is included into the fit for consistency. Spectra II and III correspond to a larger initial coverage (>2ML), acquired directly after adsorption (III) and long time irradiation (II). These spectra illustrate the decomposition with increasing photon dose. With SO_2 adsorbed on graphene/Ir(111), all fragments (SO and S) are present shortly after the irradiation has started. With subsequent photon dose, SO_2 and S components vanish, leaving mostly the SO line in the spectrum, whose intensity corresponds here to an amount of sulfur of about 9% with respect to the C $1s$ intensity. It is sensible to assume that the more SO_2 is present after adsorption, the more SO fragments are then present after oxidation. These fragments may be adsorbed on graphene in those areas which are rehybridized towards sp^3. This may also explain the larger ratio of peaks B and C in Figure 1. SO fragments chemisorbed on graphene may further distort the graphene backbone due to their potential chemical interaction, inducing more sp^3 rehybridized carbon atoms.

Such a perturbation of the graphene backbone should be visible in the substrate NEXAFS at the carbon K edge, resulting from the oxidation and possibly scaling with the amount of SO_2 on the surface. Figure 3 shows the NEXAFS spectra obtained for clean graphene/Ir(111) (black), graphene oxide obtained from a small (blue) and graphene from a large initial coverage of SO_2 (red). α is the angle between the incident light and the surface normal. We have interpreted the changes in the C $1s$ core level line shape above (Figure 1) as being due to changes in hybridization. Upon rehybridization, e.g. by a transition from sp^2-carbon to sp^3-carbon, the former sp^2 configuration of the π^* states of graphene is perturbed towards a tetrahedral structure. It is well known [9] that this process leads to a reduction in intensity of the NEXAFS line at ~285 eV photon energy and a broadening; the C $1s \rightarrow \sigma^*$ transition is broadened as well. The weakening of the C $1s \rightarrow \pi^*$ transition at $\alpha = 50\,^\circ$ coincides with an enhancement of the same signal at $\alpha = 0\,^\circ$. Because of rehybridization, the formerly almost perfectly planar p_z orbitals of the graphene layer are distorted towards a tetrahedral sp^3 state. While in perfectly planar graphene, the C $1s \rightarrow \pi^*$ transition is forbidden at normal incidence ($\alpha = 0°$), on account

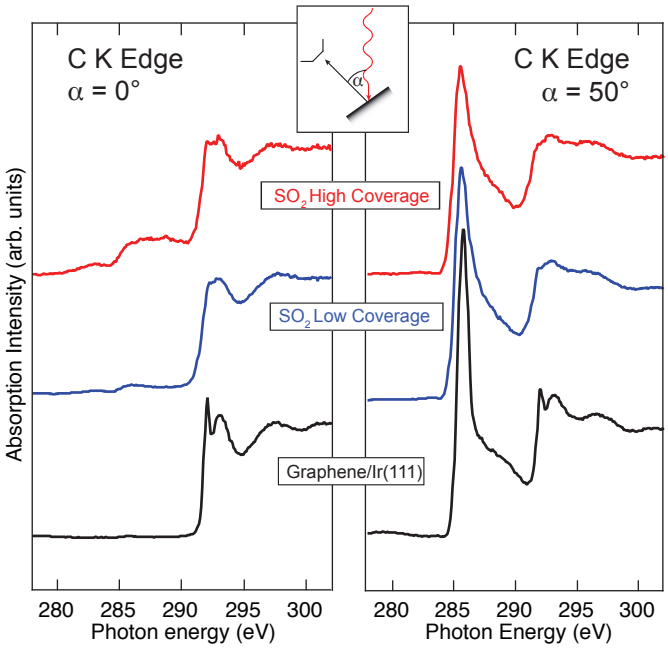

Figure 3: NEXAFS spectra for pristine graphene/Ir(111) (black), GrO/Ir(111) formed from SO_2 adsorption with a low (blue) and high (red) initial coverage. The spectra are acquired for two different angles of incident light: $\alpha = 0\,^\circ$ for normal incident light and $\alpha = 50\,^\circ$.

of dipole selection rules (the so-called searchlight effect [17]), the distortion towards sp^3 breaks the symmetry and the transition becomes allowed. Compared to pristine graphene, the NEXAFS signal at 285 eV photon energy exhibits an enhancement by a factor of 6 in graphene oxide (measured from the area under the the spectrum in the range of 284.5 to 287.5 eV) prepared here by SO_2 adsorption and photodissociation (some intensity in this region in pristine graphene is assigned to the corrugation of the moiré structure of graphene on Ir(111) and the resulting deviation from a perfect structure). The general trend seen in Figure 3 is similar to our recent results for NO_2 adsorption[12].

Apart from the broadening of the transition around 285 eV photon energy, the spectrum is also much broader in the energy range between the C $1s \rightarrow \pi^*$ and the C $1s \rightarrow \sigma^*$ transitions around 288 eV. We interpret this broadening to reflect the discussed strong influence of the SO fragments on the graphene backbone, besides the oxidation and its related rehybridization. One explanation may be the fact that we find SO_2 fragments remaining on the surface. The majority of the remaining fragments is SO. We assume that these fragments are mainly adsorbed in the vicinity of the epoxidic carbon atoms. It is well known that adsorbates tend to bind at the crystallographic areas with the highest chemical activity on the graphene/Ir(111) surface [14, 18, 19], i.e. the so-called *top-fcc* and *top-hcp* sites of the graphene/Ir(111) unit cell, where the crystallographic configuration has one carbon atom located above the surface Ir atom and one carbon atom above the crystallographic *fcc* or *hcp* hollow site of the (111) surface, respectively. Such areas are reported to show an enhanced chemical activity due to the for-

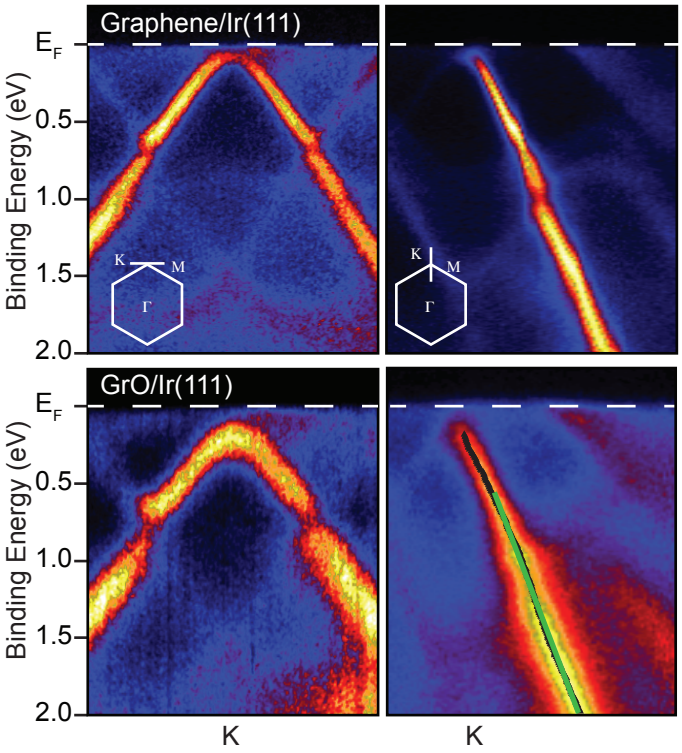

Figure 4: ARPES measurement at the K point of the hexagonal Brillouin zone for graphene/Ir(111) (upper panels) and GrO/Ir(111) (lower panels). The images are acquired perpendicular to and along the $\Gamma \rightarrow$ K direction, as illustrated by the inset Brillouin zones. The black lime superimposed in the lower right panel is the fit of the photoemission peak maximum and the green line is the linear fit of the π band dispersion.

mation of covalent bonds between the graphene and the Ir(111) substrate[14]. These bonds are similar to those reported for graphene/Ni(111) by Li *et al.* [20], for example. These authors argue that the formation of a bond between graphene and the Ni(111) surface leads to the formation of electronic states that extend away from the graphene surface into the vacuum and can act as a bonding partner towards adsorbates. Busse *et al.* [14] suggested the formation of similar electronic states in the vicinity of the *top-fcc* and *top-hcp* sites of the graphene/Ir(111) surface unit cell. Hence, it is plausible to assume that the adsorbed SO_2 molecules, the photon-induced oxidation and the remaining SO fragments are located in these areas. The observed broadening of the NEXAFS signal at $\alpha = 0\,^\circ$ may therefore result from the interaction and additional rehybridization, adjacent to the already oxidized and rehybridized carbon atoms.

In order to study the effects of the GrO formation on the electronic structure, valence band photoelectron images of GrO around the K point of the hexagonal Brillouin zone were acquired at room temperature by ARPES. Figure 4 shows such a photoemission dataset acquired for pristine graphene/Ir(111) (upper panels) and GrO/Ir(111) (lower panels). The images are presented along the $\Gamma \rightarrow$ K and perpendicular to the $\Gamma \rightarrow$ K direction as energy vs. k_x and k_y, respectively, indicated by the schematic representation of the Brillouin zone in the two upper panels. Upon oxidation, two major changes are observed. First, the π band is broadened in energy, as already observed for GrO/Ir(111) obtained by oxygen atom bombardment by Schulte *et al.* [21]. Furthermore, a band gap is formed at the K point, with a magnitude on the order of several hundred meV. In order to quantify the gap size, we assume a symmetric gap opening around the former Dirac energy, E_D. The Dirac crossing is not visible in pristine graphene/Ir(111) since it is located around 150 meV above E_F. Thus the gap cannot be measured from the maximum in the graphene (-oxide) π band alone. The former Dirac crossing energy of the oxidized graphene layer has to be calculated from an extrapolation of a linear fit of the π band dispersion in a region that is unperturbed by gap formation; this is the energy range from 0.3 to 4 eV binding energy on GrO/Ir(111). The result of the fit is presented in the lower right panel of Figure 4, as a superimposed black line on the ARPES map along $\Gamma \rightarrow$ K. The π band dispersion was obtained as follows: the electronic band peak in the momentum distribution curves along $\Gamma \rightarrow$ K was fitted by a Lorentzian profile, and this fit was performed for every momentum distribution curve for each energy level of the spectrum along the $\Gamma \rightarrow$ K direction. The result is the black line in the lower right panel of Figure 4 that follows the maximum intensity of the peak in the spectrum, i.e. the dispersion of the π band. This dispersion was then fitted by a linear function (green line in Figure 4), allowing to interpolate the former Dirac energy at the K point. The gap was then assumed to be twice the energy difference between the maximum of the π band and the former E_D at the K point, resulting in an energy gap of 330 ± 60 meV between the valence and conduction band, a value that is similar to other oxidized graphene layers [21]. The overall symmetry of the graphene overlayer has apparently not changed, since the replica bands and the mini-gaps, caused by the superpotential of the graphene/Ir(111) moiré [22] are still present.

The formation of graphene oxide by adsorption and decomposition of SO_2 is completely reversible at elevated temperatures (approx. 500 °C), yielding graphene of high quality. This was already found in our recent publication for the oxidation of graphene/Ir(111) by adsorption and decomposition of NO_2[12]. Since graphene oxide prepared by the method shown here contains epoxidic oxygen only, the reduction towards graphene oxide does not induce defects, as recently shown by Larciprete *et al.* [11].

4. Conclusions

We have demonstrated that SO_2 can be utilized to oxidize graphene adsorbed on Ir(111). Similar to NO_2 [12], the reaction is selective to the formation of epoxidic oxygen. Upon oxidation, graphene shows a clear rehybridization and the corresponding changes in the substrate NEXAFS. In addition, the adsorbed decomposition product SO further distorts the graphene backbone. We observe here the effect of a considerably strong interaction of graphene with the SO fragments. The activated (rehybridized) areas adjacent to the epoxide groups are thought to provide adsorption sites for SO, which enhances the distortion. Graphene oxide obtained by this method is stable at room temperature and shows a band gap of 330 ± 60 meV.

Acknowledgment

We would like to acknowledge W. Mahler and B Zada and the staff of BESSY II, and support through the European Science Foundation under the EUROCORES "Euro GRAPHENE" program, project SpinGraph, the Deutsche Forschungsgemeinschaft (DFG) through the Schwerpunktprogramm 1459 "Graphene", and projects HO797/18-1 and DE1679/2-1.

[1] R. J. Koch, M. Weser, W. Zhao, F. Viñes, K. Gotterbarm, S. M. Kozlov, O. Höfert, M. Ostler, C. Papp, J. Gebhardt, H. P. Steinrück, A. Görling, T. Seyller, Phys. Rev. B 86 (2012) 075401.
[2] J. Sofo, A. Chaudhari, G. Barber, Phys. Rev. B 75 (2007) 153401.
[3] D. C. Elias, R. R. Nair, T. Mohiuddin, S. V. Morozov, P. Blake, M. P. Halsall, A. C. Ferrari, D. W. Boukhvalov, M. I. Katsnelson, A. K. Geim, Science 323 (2009) 610–613.
[4] R. R. Nair, W. Ren, R. Jalil, I. Riaz, V. G. Kravets, L. Britnell, P. Blake, F. Schedin, A. S. Mayorov, S. Yuan, M. I. Katsnelson, H.-M. Cheng, W. Strupinski, L. G. Bulusheva, A. V. Okotrub, I. V. Grigorieva, A. N. Grigorenko, K. S. Novoselov, A. K. Geim, Small 6 (2010) 2877–2884.
[5] A. L. Walter, H. Sahin, K.-J. Jeon, A. Bostwick, S. Horzum, R. Koch, F. Speck, M. Ostler, P. Nagel, M. Merz, S. Schupler, L. Moreschini, Y. J. Chang, T. Seyller, F. M. Peeters, K. Horn, E. Rotenberg, ACS Nano (accepted 2014).
[6] D. Boukhvalov, M. Katsnelson, A. Lichtenstein, Phys. Rev. B 77 (2008) 035427.
[7] Y. Zhu, S. Murali, W. Cai, X. Li, J. W. Suk, J. R. Potts, R. S. Ruoff, Adv. Mat. 22 (2010) 3906–3924.
[8] W. S. Hummers, Jr, R. E. Offeman, J. Am. Chem. Soc. 80 (1958) 1339–1339.
[9] N. A. Vinogradov, K. Schulte, M. L. Ng, A. Mikkelsen, E. Lundgren, N. Mårtensson, A. B. Preobrajenski, J. Phys. Chem. C 115 (2011) 9568–9577.
[10] M. Z. Hossain, J. E. Johns, K. H. Bevan, H. J. Karmel, Y. T. Liang, S. Yoshimoto, K. Mukai, T. Koitaya, J. Yoshinobu, M. Kawai, A. M. Lear, L. L. Kesmodel, S. L. Tait, M. C. Hersam, Nat. Chem. 4 (2012) 305–309.
[11] R. Larciprete, S. Fabris, T. Sun, P. Lacovig, A. Baraldi, S. Lizzit, J. Am. Chem.l Soc. 133 (2011) 17315–17321.
[12] S. Böttcher, H. Vita, K. Horn, Surf. Sci. 621 (2014) 117–122.
[13] W. Mahler, unpublished, 2012.
[14] C. Busse, P. Lazić, R. Djemour, J. Coraux, T. Gerber, N. Atodiresei, V. Caciuc, R. Brako, A. T. N'Diaye, S. Blügel, J. Zegenhagen, T. Michely, Phys. Rev. Lett. 107 (2011) 036101.
[15] M. Polcik, L. Wilde, J. Haase, B. Brena, G. Comelli, G. Paolucci, Surf. Sci. 381 (1997) L568–L572.
[16] M. Polcik, L. Wilde, J. Haase, B. Brena, D. Cocco, G. Comelli, G. Paolucci, Phys. Rev. B 53 (1996) 13720.
[17] J. Stöhr, D. A. Outka, Phys. Rev. B 36 (1987) 7891–7905.
[18] P. Feibelman, Phys. Rev. B 77 (2008) 165419.
[19] J. Knudsen, P. J. Feibelman, T. Gerber, E. Grånäs, K. Schulte, P. Stratmann, J. N. Andersen, T. Michely, Phys. Rev. B 85 (2012) 035407.
[20] X. Li, J. Feng, E. Wang, S. Meng, J. Klimeš, A. Michaelides, Phys. Rev. B 85 (2012) 085425.
[21] K. Schulte, N. A. Vinogradov, M. L. Ng, N. Mårtensson, A. B. Preobrajenski, Appl. Surf. Sci. 267 (2013) 74–76.
[22] I. Pletikosić, M. Kralj, P. Pervan, R. Brako, J. Coraux, A. N'diaye, C. Busse, T. Michely, Phys. Rev. Lett. 102 (2009) 056808.